Diversity Analysis for Spatial Scattering Modulation in Millimeter Wave MIMO System

Shengzhen Ruan*, Bin Hu*, Kyeong Jin Kim†, Qiang Li‡, Lei Yuan*, Long Jin*, and Jiliang Zhang§
*School of Information Science and Engineering, Lanzhou University, Lanzhou, China.
†Mitsubishi Electric Research Lab (MERL), Cambridge, MA, USA.
‡School of Electronic Information and Communications, Huazhong University of Science and Technology, Wuhan, China.
§Department of Electronic and Electrical Engineering, The University of Sheffield, Sheffield, UK.
e-mail: jiliang.zhang@sheffield.ac.uk

***Abstract*—In this paper, the asymptotic average bit error probability (ABEP) is analytically analyzed for a spatial scattering modulation (SSM) in millimeter-wave (mmWave) MIMO system. An asymptotic union upper bound on the ABEP of the SSM system is obtained in a closed-form. On this basis, the achievable diversity gain of the SSM system is characterized. Simulation results demonstrate the tradeoff between spectral efficiency and ABEP performance, where the impacts of wireless channel properties and modulation order on the performance of SSM systems are investigated.**

***Index Terms*—Millimeter wave, Spatial scattering modulation, Average bit error probability, Diversity gain**

I. Introduction

Multiple Input Multiple Output (MIMO) technologies, which achieve a high spectral efficiency, have gained widespread attention in recent decades. However, employing multiple antennas increases the system complexity due to inter-channel interference (ICI) [1]–[3]. Recently, single-radio-frequency-based MIMO techniques, e.g., spatial modulation (SM), were proposed, where only one antenna element in an antenna array is activated for data transmission at any signaling time instance [4]–[8].

In the past decade, SM systems have been widely investigated. In [9], an optimal detector was derived for the SM system, where it shows that the system performance can be further improved compared to the conventional demodulator [5]. The authors in [10]–[12] derived the numerical average bit error probability (ABEP) of the SM system over various fading channels. The authors in [13] evaluated the performance over generalized fading channels, for which a comprehensive analytical framework is derived to compute the ABEP under general modulation schemes and correlated fading channels. The performance of SM systems are validated via practical measurements [14], [15]. Furthermore, the SM scheme has been generalized by combining other concepts, such as the space shift keying (SSK) [16]–[20], the generalized SM (GSM) [3], the polarization shift keying system [24], [25] and the quadrature spatial modulation (QSM) [21]–[23]. In conclusion, recent studies have demonstrated that SM can be a promising wireless communication technique.

However, some challenges and limitations need to be addressed before its widespread application in practical environment [1]. while much higher data rate demand is leading to saturating the microwave spectrum, more and more attention has been paid to the millimeter-wave (mmWave) because of its broad range of idle frequencies still existing [26]. Due to the sensitivity of mmWave to the blockages, mmWave frequencies show more severe propagation loss than the microwave counterparts under the Line-of-Sight (LoS). To resolve the severe path loss for mmWave bandwidth, large antenna arrays are required to steer a high beamforming gain. Thus, it is a great challenge to design an innovative transceiver architecture. Recently, a novel single-radio-frequency (RF) MIMO scheme was proposed, called the spatial scattering modulation (SSM) [27]. Practically, this new modulation scheme is designed for mmWave systems, whose basic idea is similar to it of SM. In the SSM scheme, it is supposed that there are N_{ts} scattering clusters with different complex gains in the propagation, among which only $N_{\mathrm{s}} \leq N_{\mathrm{ts}}$ scattering clusters with larger complex gains are available to transmit signals. In each time slot, the transmitter forms a narrow and directional beam to transmit toward only one of these available scattering clusters, while an additional information is modulated on the direction of the beam toward the N_{s} clusters, so the transmission rate is $\log_2 N_{\mathrm{s}} M$ bits per transmission, where M denotes modulation order of conventional signal constellation, e.g., M-phase-shift-keying (M-PSK) or M-quadrature-amplitude-modulation (M-QAM). Besides, an upper bound on the ABEP of the SSM is derived and the corresponding performance in various environment is analytically investigated in [27]. However, its numerical results are required precisely through more than 10^5 realizations, which is too time-consuming for analytical simulation [13].

In this paper, we derive the pairwise error probability (PEP), a tight upper bound on the ABEP, then an asymptotic upper bound on the ABEP, consequently. From the asymptotic upper bound, the diversity gain of SSM system is derived as $N_{\mathrm{ts}} - N_{\mathrm{s}} + 1$, while assuming the channel has N_{ts} scatters and N_{s} of them are employed to convey information. To justify the theoretical results, we compare them with the Monte-Carlo simulations and the original analytical ABEP expression provided by [27]. In addition, we compare the asymptotic performance of SSM systems with various modulation parameters, i.e., N_{s} and M under enviroments with different N_{ts}.

The remainder of this paper is organized as follows. Section II proposes the system model of the SSM. Based on the

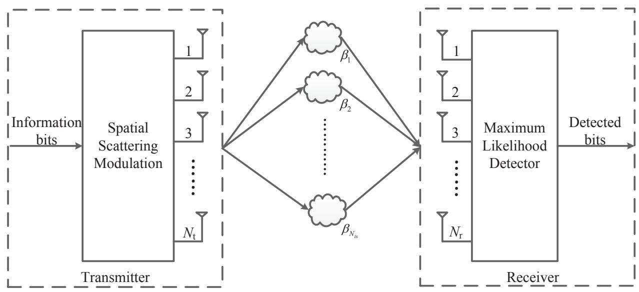

Fig. 1. The system model of SSM. Only a single RF chain is utilized at transmitter to achieve direction selection, while multiple RF chains at receiver to achieve direction detection.

definition of ABEP in [27], we derive the closed-form ABEP union upper bound in Section III. And then, we obtain the asymptotic ABEP in the high signal-to-noise ratio (SNR) regime, then extract the diversity gain in Section IV. In Section V, we analyze the performance of SSM system for various setups. Finally, we conclude the paper.

In this paper, we adopt a complex envelope signal representation. Superscript $(\cdot)^{\mathrm{H}}$ is used to denote Hermitian matrix transposition. $\mathrm{E}(\cdot)$ and $||\cdot||^2$ respectively denote the expectation and L_2 norm. ρ is the average signal to noise ratio (SNR) for each transmission. $\hat{\cdot}$ is the estimated message by the detector. $x!$ is the factorial of x.

II. Spatial Scattering Modulation

The system model of SSM is shown in Fig.1, which consists of N_{t} transmit antennas, N_{r} receive antennas, and N_{ts} scattering clusters. Since the signal is transmitted toward one out of N_{ts} scattering clusters and goes over an $N_{\mathrm{r}}\times N_{\mathrm{t}}$ wireless channel $\mathbf{H}$, the channel matrix of the SSM system can be written as a sum of N_{ts} sub-channel matrices [28]:

$$\mathbf{H}=\sum_{l=1}^{N_{\mathrm{ts}}}\beta_l\mathbf{h}_{r,l}\mathbf{h}_{t,l}^{\mathrm{H}},\tag{1}$$

where β_l denotes the complex gain of the lth scattering cluster, $\beta_l\sim CN(0,1)$. $\mathbf{h}_{t,l}$ denotes the directional vector from transmit antenna to the lth cluster, and $\mathbf{h}_{r,l}$ denotes the directional vector the beam arrives at receiver. The directional vectors $\mathbf{h}_{t,l}$ and $\mathbf{h}_{r,l}$ are expressed as those in [27]. When we assume that the array of antenna is large enough, the directional vectors will be approximately orthogonal, i.e., $\mathbf{h}_{t,l}^{\mathrm{H}}\mathbf{h}_{t,k}\approx 0$ and $\mathbf{h}_{r,l}^{\mathrm{H}}\mathbf{h}_{r,k}\approx 0$ when $l\neq k$, and $\mathbf{h}_{t,l}^{\mathrm{H}}\mathbf{h}_{t,k}\approx 1$ and $\mathbf{h}_{r,l}^{\mathrm{H}}\mathbf{h}_{r,k}\approx 1$ when $l=k$. According to the SSM scheme, the received signal can be written as:

$$\mathbf{y}=\sqrt{\rho}\mathbf{H}\mathbf{p}_k s_m+\mathbf{n},\tag{2}$$

where $\mathbf{p}_k$ denotes the directional vector from the transmitter to the k-th scattering cluster, $1\leq k\leq N_{\mathrm{s}}$, s_m is the m-th signal of the conventional signal constellation diagram, $1\leq m\leq M$, and $\mathbf{n}\sim CN(0,1)$ is the $N_{\mathrm{r}}\times 1$ dimensional white Gaussian noise vector.

Exploit the orthogonality of the directional vectors and apply the maximum likelihood detector to estimate the direction and the received symbol, the detection rule is expressed as follows:

$$\begin{aligned}\left[\hat{k},\hat{m}\right]&=\underset{k,m}{\arg\min}\,\|\mathrm{y}_{\mathrm{c}}(k)-h_{r,k}^{\mathrm{H}}\sqrt{\rho}\mathrm{H}h_{t,k}s_m\|^2\\&=\underset{k,m}{\arg\min}\,\|\mathrm{y}_{\mathrm{c}}(k)-\sqrt{\rho}\beta_k s_m\|^2,\end{aligned}\tag{3}$$

where $\hat{k}$ and $\hat{m}$ denote indexes of estimated direction and estimated symbol, respectively. Note that when $k=\hat{k}$, $\mathbf{y}_c(k)=\mathbf{h}_{r,k}\mathbf{n}+\sqrt{\rho}\beta_k s_m$, whereas when $k\neq\hat{k}$, $\mathbf{y}_c(k)=\mathbf{h}_{r,k}\mathbf{n}$.

III. Closed-Form Union Upper Bound on ABEP

A. Union Upper Bound

For a fast and exact evaluation of the SSM system, we need to derive the closed-form PEP based on the original ABEP. The performance of the SSM system is upper bounded as [27, Eq. (11)]

$$\begin{aligned}\mathrm{ABEP}\leq&\sum_{k=1}^{N_{\mathrm{s}}}\sum_{m=1}^{M}\sum_{\hat{k}=1}^{N_{\mathrm{s}}}\sum_{\hat{m}=1}^{M}\\&\times\frac{N\left([k,m]\to[\hat{k},\hat{m}]\right)P\left([k,m]\to[\hat{k},\hat{m}]\right)}{N_{\mathrm{s}}M\log_2(N_{\mathrm{s}}M)},\end{aligned}\tag{4}$$

where $N\left([k,m]\to[\hat{k},\hat{m}]\right)$ denotes the Hamming distance between $[k,m]$ and $[\hat{k},\hat{m}]$, and $P\left([k,m]\to[\hat{k},\hat{m}]\right)$ denotes the PEP, which is the probability of detecting $[k,m]$ as $[\hat{k},\hat{m}]$. In [27], the PEP is given by:

$$\begin{aligned}&P\left([k,m]\to[\hat{k},\hat{m}]|\beta_k,\beta_{\hat{k}}\right)\\&=\begin{cases}Q\left(\sqrt{\dfrac{\rho}{2}|\beta_k(s_m-s_{\hat{m}})|^2}\right) & ,k=\hat{k},\\ \dfrac{1}{2}e^{-\frac{\rho}{2}|\beta_{\hat{k}}|^2|s_{\hat{m}}|^2} & ,k\neq\hat{k}.\end{cases}\end{aligned}\tag{5}$$

Note that the PEP in (5) is determined by the specific realization of the Log-Normal distributed $|\beta_k|^2$. Thus for fast evaluation of the SSM system, we calculate the expected PEP of the SSM system, $\mathrm{E}\left[P\left([k,m]\to[k,\hat{m}]|\beta_k,\beta_{\hat{k}}\right)\right]$.

B. Closed-form expression for the PEP with $k=\hat{k}$

We assume that the complex gain $\beta_l\sim CN(0,1)$, and $|\beta_l|^2$ is exponentially distributed with a probability density function (PDF) of $f(x)=e^{-x}$, and a cumulative distribution function (CDF) of $F(x)=1-e^{-x}$. Without loss of generality, the magnitude of the complex gain $|\beta_l|^2$ is sorted in a decreasing order, i.e., $|\beta_1|^2>|\beta_2|^2>\cdots>|\beta_{N_{ts}}|^2$. Thus, the random variable $|\beta_k|^2$ is an order statistic [31] with a PDF of

$$f_{\beta_k}(x)=\frac{N_{\mathrm{ts}}!\left(1-e^{-x}\right)^{N_{\mathrm{ts}}-k}\left(e^{-x}\right)^k}{(N_{\mathrm{ts}}-k)!(k-1)!}.\tag{6}$$

From (6), using binomial formula [29], the PDF of $|\beta_k|^2$ is rewritten as

$$f_{\beta_k}(x) = \frac{N_{\rm ts}!}{(k-1)!}\sum_{r=0}^{N_{\rm ts}-k}\frac{(-1)^r e^{-(r+k)x}}{r!(N_{\rm ts}-k-r)!}. \tag{7}$$

Substituting

$$Q(x) = \frac{1}{\pi}\int_0^{\pi/2}\exp[-x^2/(2\sin^2\phi)]d\phi \tag{8}$$

in to (5), the closed-form expression for the PEP with $k=\hat{k}$ is derived as follows:

$$\begin{aligned}\mathrm{E}\left[P\left([k,m]\to[k,\hat{m}]|\beta_k\right)\right] &= \mathrm{E}\left[Q\left(\sqrt{\frac{\rho}{2}|s_m - s_{\hat{m}}|^2 x}\right)\right]\\ &= \int_0^\infty \frac{1}{\pi}\int_0^{\frac{\pi}{2}}\exp\left(-\frac{\rho|s_m-s_{\hat{m}}|^2 x}{4\sin^2\phi}\right)\mathrm{d}\phi f_{\beta_k}(x)\mathrm{d}x.\end{aligned} \tag{9}$$

Substituting (7) into (9), the closed-form expression for the PEP for $k=\hat{k}$ is evaluated as follows:

$$\begin{aligned}&\mathrm{E}\left[P\left([k,m]\to[k,\hat{m}]|\beta_k\right)\right]\\ &= \frac{N_{\rm ts}!}{(k-1)!}\sum_{r=0}^{N_{\rm ts}-k}\frac{(-1)^r\left(1-\sqrt{\frac{\rho|s_m-s_{\hat{m}}|^2}{\rho|s_m-s_{\hat{m}}|^2+4(r+k)}}\right)}{r!(N_{\rm ts}-k-r)!2(r+k)}.\end{aligned} \tag{10}$$

C. Closed-form expression for the PEP with $k \neq \hat{k}$

For $k \neq \hat{k}$, the PEP is determined by $|\beta_{\hat{k}}|^2$, whose PDF is given by (7). From (5), following some straightforward algebraic manipulations, the PEP for $k \neq \hat{k}$ is derived as follows:

$$\begin{aligned}&\mathrm{E}\left[P\left([k,m]\to[\hat{k},\hat{m}]|\beta_{\hat{k}}\right)\right]\\ &= \frac{N_{\rm ts}!}{2(\hat{k}-1)!}\sum_{r=0}^{N_{\rm ts}-\hat{k}}\frac{(-1)^r}{r!(N_{\rm ts}-\hat{k}-r)!(\frac{\rho}{2}|s_{\hat{m}}|^2+r+\hat{k})}.\end{aligned} \tag{11}$$

Substituting (10) and (11) into (4), we obtain the closed-form upper bound on the ABEP of the SSM systems.

IV. Diversity Gain Analysis

In this section, the achievable diversity gain and coding gain of the considered SSM system is investigated based on the analytically obtained ABEP in the previous section. For $k=\hat{k}$, we suppose and define $N = N_{\rm ts}-k+1$, the PEP can be approximated as:

$$\begin{aligned}&\mathrm{E}\left[P\left([k,m]\to[k,\hat{m}]|\beta_k\right)\right]\\ &\doteq \frac{(\rho|s_m-s_{\hat{m}}|^2)^{-N}(2N-1)!!N_{\rm ts}!}{2^{2N+1}(2N)!!(k-1)!},\end{aligned} \tag{12}$$

where $(2N)!! = 2\times4\times6\times\cdots\times(2N)$, and $(2N-1)!! = 1\times3\times5\times\cdots\times(2N-1)$. See Appendix A for the derivation.

For $k \neq \hat{k}$, as the SNR increases, the parameter r in the denominator of (11) can be ignored. Hence, the PEP can be approximated as:

$$\begin{aligned}&\mathrm{E}\left[P\left([k,m]\to[\hat{k},\hat{m}]|\beta_{\hat{k}}\right)\right]\\ &\doteq \frac{N_{\rm ts}!\left(|s_{\hat{m}}|^{-2(N_{\rm ts}-\hat{k}+1)}\right)\rho^{-(N_{\rm ts}-\hat{k}+1)}}{2^{N_{\rm ts}-\hat{k}+2}(\hat{k}-1)!}.\end{aligned} \tag{13}$$

See Appendix B for the derivation of (13).

Substituting (12) and (13) into the union upper bound, an asymptotic ABEP can be expressed as:

$$\mathrm{ABEP} \doteq \sum_{k=1}^{N_{\rm s}}\sum_{m=1}^{M}\sum_{\hat{k}=1}^{N_{\rm s}}\sum_{\hat{m}=1}^{M}\rho^{-(N_{\rm ts}-k+1)}G(k,m,\hat{k},\hat{m}), \tag{14}$$

where $G(k,m,\hat{k},\hat{m})$ is defined as:

$$\begin{aligned}G(k,m,\hat{k},\hat{m}) &= \frac{N\left([k,m]\to[\hat{k},\hat{m}]\right)N_{\rm ts}!}{2N_{\rm s}M\log_2(N_{\rm s}M)(k-1)!}\\ &\times\begin{cases}\dfrac{4^{N_{\rm ts}-k+1}(2N-1)!!}{|s_m-s_{\hat{m}}|^{2(N_{\rm ts}-k+1)}(2N)!!} & ,k=\hat{k},\\ \dfrac{2^{(N_{\rm ts}-k+1)}}{s_{\hat{m}}^{2(N_{\rm ts}-k+1)}} & ,k\neq\hat{k}.\end{cases}\end{aligned} \tag{15}$$

In the high SNR regime, the worst term in (14) dominates the slope of the ABEP [32] and therefore, we have the asymptotic ABEP as:

$$\mathrm{ABEP}_{\rm asym} = (\mathcal{C}\rho)^{-\mathcal{D}}, \tag{16}$$

where the diversity gain is

$$\mathcal{D} = N_{\rm ts} - N_{\rm s} + 1, \tag{17}$$

whereas, the coding gain is

$$\mathcal{C} = \left[\sum_{m=1}^{M}\sum_{\hat{k}=1}^{N_{\rm s}}\sum_{\hat{m}=1}^{M}G(N_{\rm s},m,\hat{k},\hat{m})\right]^{-\frac{1}{\mathcal{D}}}. \tag{18}$$

V. Numerical Results

In this section, we carry out numerical experiments, and compare the performance of the SSM systems for various values of $N_{\rm s}$ and $N_{\rm ts}$. Meanwhile, we compare the SSM scheme with two benchmark schemes: maximum beamforming (MBF), where the transmitter only transmits the signal toward the scattering cluster having the largest gain β_1, and random beamforming (RBF) where the transmitter transmits the signal to one of $N_{\rm s}$ clusters randomly [27]. For a fair comparison, we fix the spectral efficiency of different schemes as four bits per channel use. Therefore, the SSM employs $N_{\rm s}=4$ scattering clusters, as well as quadrature phase shift keying (QPSK) mapper. As the scattering clusters of the MBF and RBF do not carry information bits, they employ 16 quadrature amplitude modulation (16-QAM).

Fig.2 shows the comparison of the exact, the original and the asymptotic ABEP curves, as well as the Monte-Carlo results.

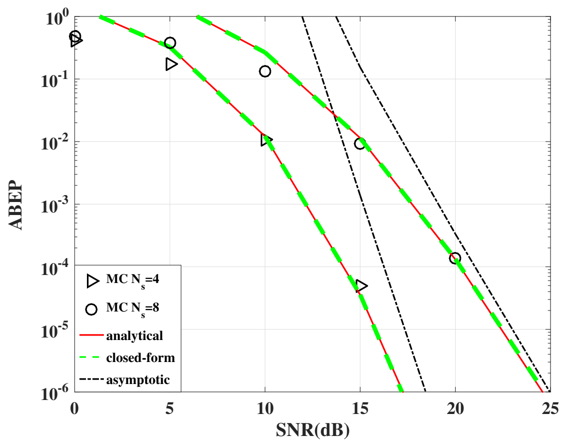

Fig. 2. Validation of analytic results via comparison of analytic results and simulations, where $N_{\mathrm{ts}} = 12$ and MC denotes Monte-Carlo results.

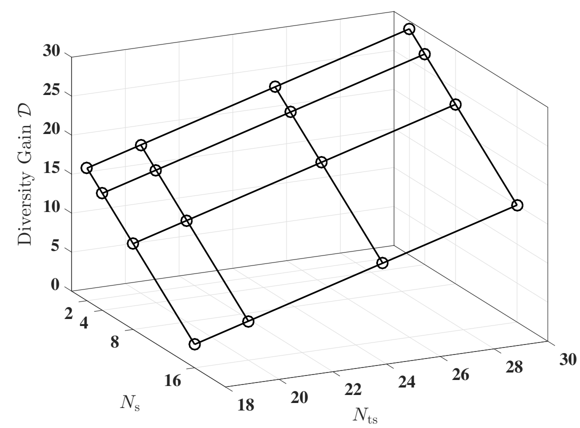

Fig. 4. Diversity gain comparison of SSM with different values of N_{s} and N_{ts}.

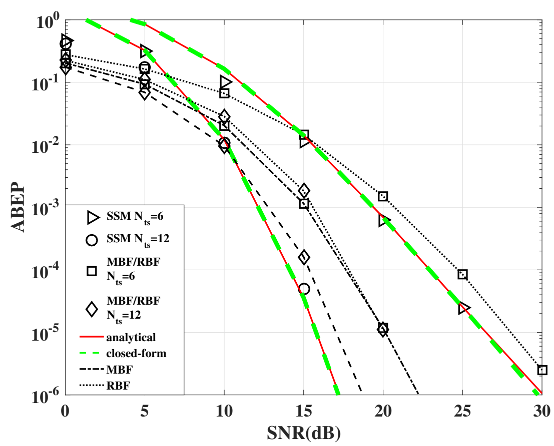

Fig. 3. ABEP performance comparison among SSM, MBF and RBF, where spectral efficiency is four bits per channel use.

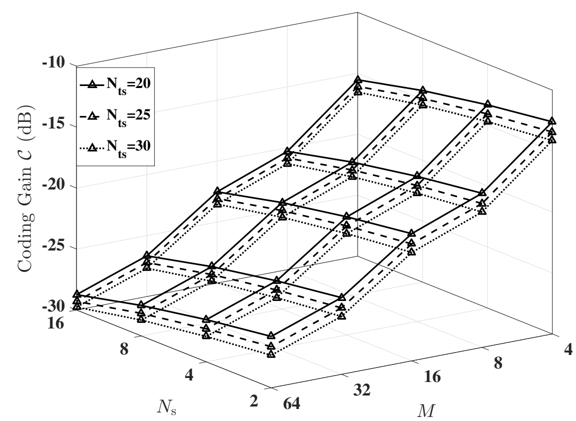

Fig. 5. Coding gain comparison of SSM with different values of N_{s}, N_{ts} and M.

We can see that the upper bound derived in (4) is tight. And the asymptotic ABEP curve approaches that of the analytical ABEP curve as the SNR increases. From the measurement, the slope of the asymptotic ABEP curve equals to $-(N_{\mathrm{ts}}-N_{\mathrm{s}}+1)$. Thus, as the N_{s} decreases, the slope of the asymptotic ABEP curve gets steeper, which leads to a better performance with other parameters being the same. In Fig.2, it is observed that the SSM system with $N_{\mathrm{s}} = 4$ achieves a better performance than the system with $N_{\mathrm{s}} = 8$.

Fig.3 demonstrates the performance comparisons among SSM, MBF and RBF. Clearly, the SSM scheme achieves a better ABEP performance when $N_{\mathrm{ts}} = 12$. From the perspective of the diversity gain, the higher diversity gain is obtained, the better system performance or higher spectral efficiency is achieved. In other word, it is found that as N_{ts} increases, a greater diversity gain is achievable. Otherwise, at a same value of N_{ts}, a higher spectral efficiency is achieved by increasing the number of N_{s}, whereas the diversity gain is decreased. For intuitive analysis, we show the diversity gain against N_{ts} and N_{s} in Fig.4. Furthermore, from Fig.5 we can clearly see that the coding gain of the SSM decreases as the modulation order or the number of N_{s} increases, where M-QAM is employed. Thus, under the same data rate, it is necessary to consider the setup of the SSM carefully.

VI. Conclusion

In this paper, a tight upper bound on the ABEP of SSM systems has been analytically derived in a closed-form expression and validated with simulations under different wireless channel properties and modulation orders. The maximum achievable diversity gain has been derived analytically. Numerical results have demonstrated that the ABEP of the SSM system decreases with increasing modulation order and the number of scatters in the surrounding environment, while a decreasing number of scatters that convey information contributes to a better performance. In other words, a tradeoff between the diversity gain and the spectral efficiency has been found.

APPENDIX

A. Derivation of Equation (12)

Since the random variable is an order statistic, we exploit the closed-form PEP with $k = \hat{k}$ in (9) to derive the approximate PEP. From (9), by exchanging the order of integration and employing [31, Eq. (2.5)], the approximate PEP can be rewritten as:

$$\begin{aligned} &\mathrm{E}\left[P\left([k,m] \to [k,\hat{m}]|\beta_k\right)\right] \\ =&\frac{1}{\pi}\int_0^{\frac{\pi}{2}} \prod_{r=k}^{N_{\mathrm{ts}}} \frac{\sin^2\phi}{\frac{\rho|s_m - s_{\hat{m}}|^2}{4r} + \sin^2\phi} d\phi. \end{aligned} \tag{19}$$

In the high SNR regime, $\sin^2\phi$ in (19) is ignorable. Therefore, we have

$$\begin{aligned} &\mathrm{E}\left[P\left([k,m] \to [k,\hat{m}]|\beta_k\right)\right] \\ =&\frac{1}{\pi}\left(\prod_{r=k}^{N_{\mathrm{ts}}} \frac{4r}{\rho|s_m - s_{\hat{m}}|^2}\right)\int_0^{\frac{\pi}{2}} (\sin\phi)^{2(N_{\mathrm{ts}}-k+1)} d\phi. \end{aligned} \tag{20}$$

By applying Wallis formula for simplification [30], the PEP can be written as (12).

B. Derivation of Equation (13)

For $k \neq \hat{k}$, $|\beta_k|^2$ becomes an exponential order statistics. Then by employing [31, Eq. (2.5)], the average PEP can be rewritten as:

$$\mathrm{E}\left[P\left([k,m] \to [\hat{k},\hat{m}]|\beta_{\hat{k}}\right)\right] = \mathrm{E}\left[\frac{1}{2}e^{-\frac{\rho|s_{\hat{m}}|^2 x}{2}}\right]. \tag{21}$$

Following some straightforward derivations, we have

$$\mathrm{E}\left[P\left([k,m] \to [\hat{k},\hat{m}]|\beta_{\hat{k}}\right)\right] = \frac{1}{2}\prod_{r=\hat{k}}^{N_{\mathrm{ts}}}\left(\frac{2r}{\rho|s_{\hat{m}}|^2 + 2r}\right). \tag{22}$$

As ρ increases, r in the denominator of (22) can be ignored. Thus, the approximate PEP is derived as (13).

ACKNOWLEDGEMENT

The research is funded in part by H2020-MSCA IF-AceLSAA (752644), in part by International Science and Technology Cooperation Program of China (2017YFE0118900), and in part by Natural Science Foundation of Gansu Province, China (18JR3RA268).

REFERENCES

[1] M. Di Renzo, et al., "Spatial modulation for multiple-antenna wireless systems: a survey," *IEEE Commun. Mag.*, vol. 49, no. 12, pp. 182-191, 2011.

[2] P. Yang, et al., "Design guidelines for spatial modulation," *IEEE Commun. Surveys Tuts.*, vol. 17, no. 1, pp. 6-26, First Quart. 2015.

[3] P. Yang, et al., "Single-carrier SM-MIMO: a promising design for broadband large-scale antenna systems," *IEEE Commun. Surveys Tut.*, vol. 18, no. 3, pp. 1687-1716, 2017.

[4] M. Di Renzo, et al., "Spatial modulation for generalized MIMO: challenges, opportunities, and implementation," *IEEE Proc.*, vol. 102, no. 1, pp. 56-103, 2013.

[5] R. Mesleh, et al., "Spatial modulation," *IEEE Trans. Veh. Technol.*, vol. 57, no. 4, pp. 2228-2241, 2008.

[6] Y. Chau and S.-H. Yu, "Space modulation on wireless fading channels," *IEEE VTC*, pp. 1668-1671, 2001.

[7] H. Haas, et al., "Increasing spectral efficiency by data multiplexing using antennas arrays," *IEEE PIMRC*, pp. 610-613, 2002.

[8] R. Y. Mesleh, et al., "Spatial modulation: a new low complexity spectral efficiency enhancing technique," *Chinacom*, pp. 1-5, 2006.

[9] J. Jeganathan, et al., "Spatial modulation: optimal detection and performance analysis," *IEEE Commun. Lett.*, vol. 12, no. 8, pp. 545-547, 2008.

[10] T. Handte, et al., "BER analysis and optimization of generalized spatial modulation in correlated fading channels," *IEEE VTC*, pp. 1-5, 2009.

[11] M. Di Renzo, et al., "Performance comparison of different spatial modulation schemes in correlated fading channels," *IEEE ICC*, pp. 1-6, 2010.

[12] M. Di Renzo, et al., "Bit error probability of space modulation over Nakagami-m fading: asymptotic analysis," *IEEE Commun. Lett.*, vol. 15, no. 10, pp. 1026-1028, 2011.

[13] M. Di Renzo and H. Haas, "Bit error probability of spatial modulation (SM-MIMO) over generalized fading channels," *IEEE Trans. Veh. Technol.*, vol. 61, no. 3, pp. 1124-1144, 2012.

[14] J. Zhang, et al., "Bit error probability of spatial modulation over measured indoor channels," *IEEE Trans. Wireless Commun.*, vol. 13, no. 3, pp. 1380-1387, 2014.

[15] J. Zhang, et al., "Performance of spatial modulation with constant transmitted power under LOS and NLOS scenarios," in Proc. *IEEE ICC*, 2015.

[16] M. D. Renzo and H. Haas, "Improving the performance of space shift keying (SSK) modulation via opportunistic power allocation," *IEEE Commun. Lett.*, vol. 14, no. 6, pp. 500-502, 2010.

[17] M. Di Renzo, et al., "Space shift keying (SSK) MIMO with practical channel estimates," *IEEE Trans. Commun.*, vol. 60, no. 4, pp. 998-1012, 2012.

[18] M. Di Renzo and H. Haas, "Space shift keying (SSK) modulationwith partial channel state information: Optimal detector and performance analysis over fading channels," *IEEE Trans. Commun.*, vol. 58, no. 11, pp. 3196-3210, 2010.

[19] S. S. Ikki and R. Mesleh, "A general framework for performance analysis of space shift keying (SSK) modulation in the presence of Gaussian imperfect estimations," *IEEE Commun. Lett.*, vol. 16, no. 2, pp. 228-230, 2012.

[20] M. Di Renzo and H. Haas, "Ageneral framework for performance analysis of space shift keying (SSK) modulation for MISO correlated Nakagami-m fading channels," *IEEE Trans. Commun.*, vol. 58, no. 9, pp. 2590-2603, 2010.

[21] R. Mesleh, et al., "Quadrature spatial modulation," *IEEE Trans. Veh. Technol.*, vol. 64, no. 6, pp. 2738-2742, 2015.

[22] B. Vo, et al., " Improved quadrature spatial modulation," in *Proc. IEEE VTC-Fall 2017*, Toronto, Canada, 24-27 Sept. 2017, pp. 1-5.

[23] R. Mesleh, et al., "Differential quadrature spatial modulation," *IEEE Trans. Commun.*, vol. 65, no. 9, pp. 3810-3817, 2017.

[24] J. Zhang, et al., "Polarization shift keying (PolarSK): system scheme and performance analysis," *IEEE Trans. Veh. Tech.*, vol. 66, no. 11, pp. 10139-10155, 2017.

[25] P. Henarejos and A. I. Pŕez-Neira, "3D polarized modulation: system analysis and performance," *IEEE Trans. Commun.*, early access.

[26] J. Andrews, et al., "What Will 5G Be ?" *IEEE J. Sel. Areas. Commun*, vol. 32, no. 6, pp. 1065-1082, 2014.

[27] Y. Ding, et al., "Spatial scattering modulation for uplink millimeter-wave systems," *IEEE Commun. Lett.*, vol. 21, no. 7, pp. 1493-1496, 2017.

[28] A. Sayeed, "Deconstructing multi-antenna fading channels," *IEEE Trans. Sig. Proc.*, vol. 50, no. 10, pp. 2563-2579, 2002.

[29] N. Bourbaki, et al., "Elements of the History of Mathematics," *Springer Berlin Heidelberg*, pp. 79-85, 1994.

[30] Mikhail and Kovalyov, "Elementary combinatorial-probabilistic proof of the Wallis and Stirling formulas," *Journal of Mathematics and Statistics*, vol. 5, no. 4, pp. 408-409, 2009.

[31] P. Vellaisamy and A. Zeleke, "Exponential order statistics, the Basel problem and combinatorial identities," pp. 1-10, 2016.

[32] Z. Wang and G. B. Giannakis, "A simple and general parameterization quantifying performance in fading channels," *IEEE Trans. Commun.*, vol. 51, no. 8, pp. 1389-1398, 2003.